Thermodynamics of host-guest interactions between methylpyridinium salts and phosphonate cavitands

Daniela Menozzi[a]; Elisa Biavardi[a]; Chiara Massera[b]; Franz-Peter Schmidtchen[c]; Andrea Cornia[d]; Enrico Dalcanale[a]

[a] Dipartimento di Chimica Organica e Industriale & INSTM, Università di Parma, Parma, Italy [b] Dipartimento di Chimica Generale e Inorganica, Chimica Analitica, Chimica Fisica, Università di Parma, Parma, Italy [c] Department Chemie, Technische Universität München, Garching, Germany [d] Dipartimento di Chimica & INSTM, Università di Modena e Reggio Emilia, Modena, Italy

PLEASE SCROLL DOWN FOR ARTICLE

Taylor & Francis
Taylor & Francis Group

Thermodynamics of host–guest interactions between methylpyridinium salts and phosphonate cavitands[†]

Daniela Menozzi[a], Elisa Biavardi[a], Chiara Massera[b], Franz-Peter Schmidtchen[c], Andrea Cornia[d] and Enrico Dalcanale[a]*

[a]*Dipartimento di Chimica Organica e Industriale & INSTM, Università di Parma, Viale G.P. Usberti 17/A, 43124 Parma, Italy;* [b]*Dipartimento di Chimica Generale e Inorganica, Chimica Analitica, Chimica Fisica, Università di Parma, Viale G.P. Usberti 17/A, 43124 Parma, Italy;* [c]*Department Chemie, Technische Universität München, D-85747 Garching, Germany;* [d]*Dipartimento di Chimica & INSTM, Università di Modena e Reggio Emilia, Via G. Campi 183, 41100 Modena, Italy*

In this work, the properties of complexation of tetraphosphonate cavitands towards methylpyridinium guests were investigated via isothermal titration calorimetry (ITC). For this purpose, **Tiiii[C$_3$H$_7$, CH$_3$, Ph]**, **Tiiii[C$_3$H$_7$, H, Ph]**, **TSiiii[C$_3$H$_7$, H, Ph]** hosts and three different methylpyridinium guests were synthesised. The role of the following parameters in the host–guest complexation was investigated: (i) solvation, (ii) nature of the guest counterion, (iii) presence of substituents in the apical positions of the receptor, and (iv) P=O versus P=S bridging units. The results showed that (i) switching from dichloroethane to methanol leads to a decrease of the association constant due to the competitive nature of the solvent, (ii) the guest counterion does not affect the thermodynamics of the process, (iii) the apical methyl groups enhance the binding affinity of the receptor and (iv) the comparison between phosphonate and thiophosphonate hosts clearly demonstrates that cation–dipole interactions are necessary for binding.

Keywords: tetraphosphonate cavitands; methylpyridinium salts; host–guest complexation; ITC

1. Introduction

Phosphonate cavitands have established themselves as one of the most promising classes of molecular receptors (*1*), thanks to their diversified complexation properties, spanning from cationic species such as ammonium, methylpyridinium and inorganic salts to neutral guests such as alcohols. In particular, their complexation prowess towards methylpyridinium salts has been exploited in the generation of functional surfaces (*2, 3*) and supramolecular polymers (*4*). The key player of the whole class is the tetraphosphonate cavitand Tiiii (*5, 6*), presenting all four P=O bridging groups oriented inward with respect to the cavity (*7*) (see Chart 1). Its peculiar complexation ability is the result of three interaction modes, which can be activated either individually or in combination by the host according to the following guest requirements: (i) multiple ion–dipole interactions between the inward-facing P=O groups and the positively charged guests (*8*); (ii) single or multiple H-bonding involving the P=O groups (*9*) and (iii) CH$_3$–π interactions between an acidic methyl group present on the guest and the π-basic cavity of the host (*10*). Depending on the type and number of interactions activated, the measured K_{ass} in non-polar solvents can vary from 10^2 M^{-1} for short-chain alcohols to 10^7 M^{-1} for

methylpyridinium salts (*11*) and even higher for N,N-methylalkylammonium salts (*4*).

An understanding of the intimate features of the host–guest interactions and their thermodynamic signatures is essential in order to optimise selectivity and strength in guest uptake. In this case, ^{31}P NMR is a diagnostic tool to assess complexation in solution due to the presence on the host of four interacting P=O units. However, in the case of methylpyridinium guests, the association constants exceed the upper limit revelation of the NMR ($10 < K_{ass} < 10^4$ M^{-1}). In this situation, isothermal titration calorimetry (ITC) represents the best alternative because it can determine association constants within the range $10^2 < K_{ass} < 10^7$ M^{-1} (*12, 13*), and it provides directly the thermodynamic parameters in the form of K_{ass}, ΔH, ΔS, ΔG and ΔC_p.

This article reports an ITC study of the influence of the following parameters on the properties of complexation of the four tetraphosphonate/thiophosphonate cavitands reported in Chart 1 towards methylpyridinium guests: (i) solvation, (ii) nature of the guest counterion, (iii) presence of substituents in the apical positions of the receptor and (iv) P=O versus P=S bridging units.

Tiiii[C₃H₇, CH₃, Ph]

Tiiii[C₃H₇, H, Ph]

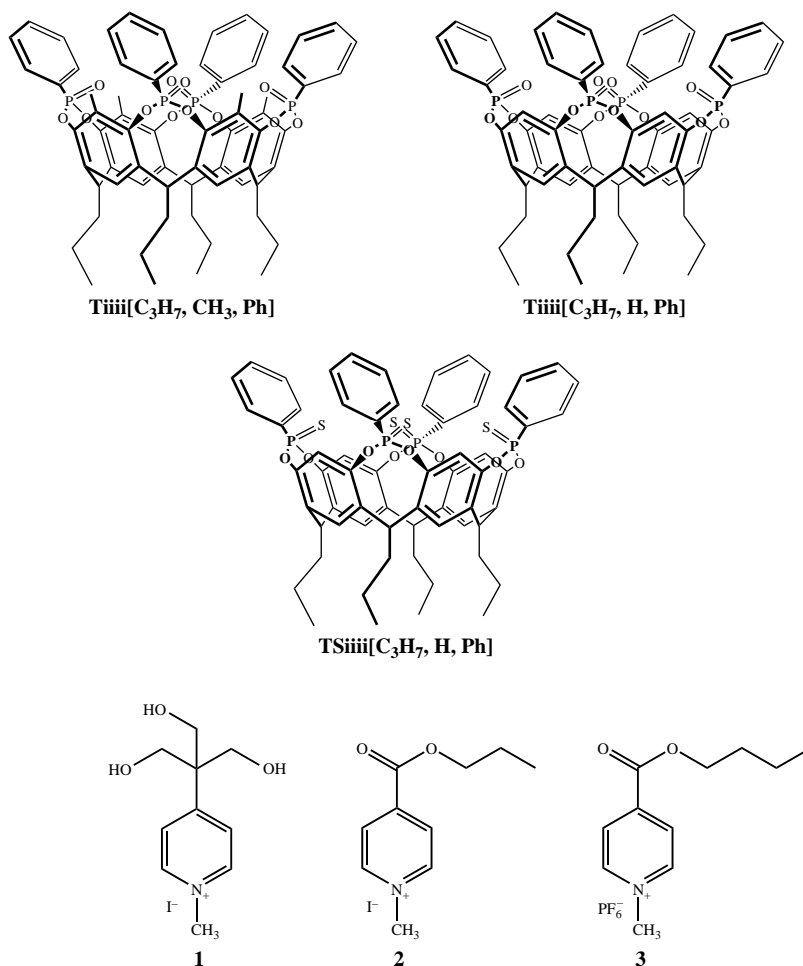**TSiiii[C₃H₇, H, Ph]**

1 **2** **3**

Chart 1. Cavitand hosts and methylpyridinium guests utilised in the present work.

2. Results and discussion

The preparation of cavitand **Tiiii[C₃H₇, CH₃, Ph]** has already been reported (*11*). Cavitands **Tiiii[C₃H₇, H, Ph]** and **TSiiii[C₃H₇, H, Ph]** were prepared via a two-step procedure. The acid-catalysed condensation between resorcinol and butyraldehyde led to the propyl-footed resorcinarene **Res[C₃H₇, H]**, which was then bridged with dichlorophenylphosphine and oxidised *in situ* either with hydrogen peroxide or with S₈ to give **Tiiii[C₃H₇, H, Ph]** and **TSiiii[C₃H₇, H, Ph]**, respectively (Scheme 1). The methylpyridinium guests **1**–**3** reported in Chart 1 were all prepared via alkylation of the corresponding pyridine precursors with methyl iodide, followed by anion exchange with NH₄PF₆ in the case of guest **3**.

The determination of the thermodynamic data from the ITC curves requires the knowledge of the binding stoichiometry of the formed complex. In our case, clearly evident 1:1 binding was in the solid state (*2*), and in solution (*11*) for ester derivatives **2**–**3** with the Tiiii hosts. For triol-substituted guest **1**, the 1:1 stoichiometry in the solid state is proven by the crystal structure of **Tiiii[C₃H₇, CH₃, Ph]·(C₁₀H₁₆INO₃)·5CH₃CN** complex (Figure 1). The presence of the four apical methyl substituents does not change stoichiometry and complexation mode with respect to the parent **Tiiii[C₂H₅, H, Ph]** cavitand (*2*).

The reported crystal structure evidences the different synergistic interactions between the tetraphosphonate cavitand **Tiiii[C₃H₇, CH₃, Ph]** and guest **1** (see Figure 1, left). The inclusion of **1** in the cavity is driven by dipolar interactions between the positively charged nitrogen atom and two P=O groups at the upper rim of the cavitand (P=O···N⁺: 3.056(3) and 3.116(3) Å). One of these P=O moieties is also involved in a hydrogen bond with an OH group of the guest (O···O=P 2.992(4) Å and O—H O=P 170.4(2)°). Further stabilisation is provided by three C—H···π interactions between the methyl hydrogens of the cation and three aromatic rings of the cavity (the C—H···centroid distances are 2.667(4), 2.828(3) and 3.129(2) Å, with angles 126.44(3), 136.15(2) and 166.64(1)°, respectively). The iodide counterion is located
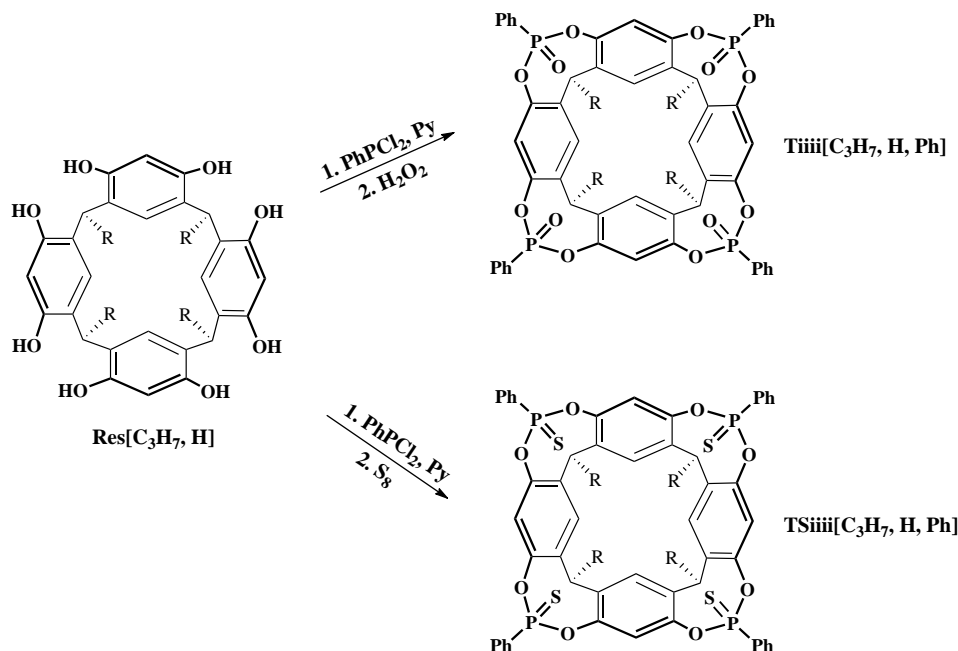
Scheme 1.   Synthesis of Tiiii[C_3H_7, H, Ph] and TSiiii[C_3H_7, H, Ph] cavitands.

below the cavity at 1.808(2) Å from the least-square plane defined by the four CH_2 carbons, roughly in the middle of the four alkyl chains at the lower rim. This position is stabilised by four C−H···I⁻ interactions with the first CH_2 groups of the chains, which range in length from 2.9985(5)

to 3.1674(5) Å. The iodide ion also forms two hydrogen bonds (one stronger and one weaker) with two OH groups of the guest of a neighbouring complex (O···I⁻ 392(2) and 3.563(4) Å; O−H···I⁻ 166.8(1) and 165.9(2)°, respectively). This influences the crystal packing which shows a
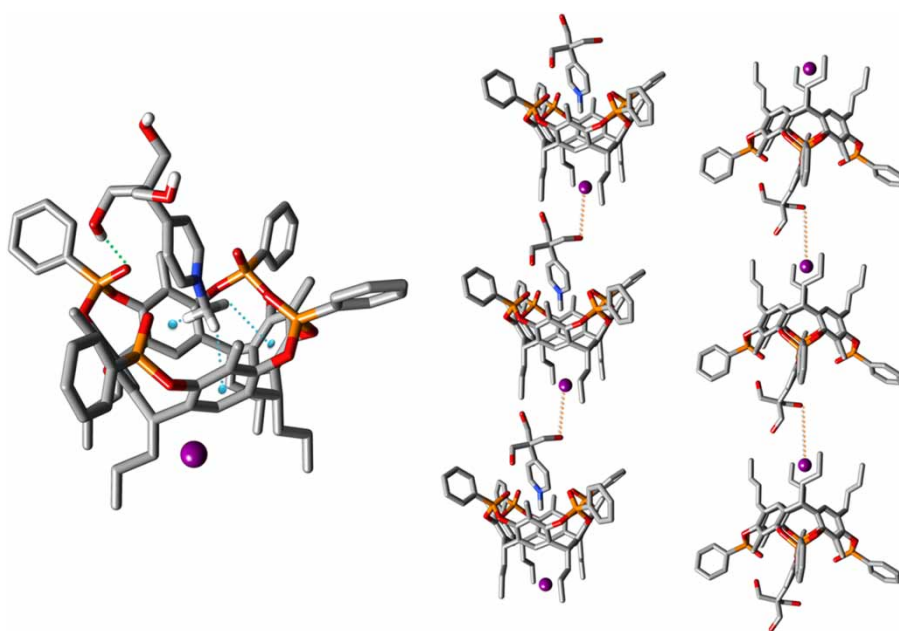
Figure 1.   Crystal structure (left) and crystal packing (right) of **Tiiii[C_3H_7, CH_3, Ph]·($C_{10}H_{16}INO_3$)·5CH_3CN** complex. Colour code: I, purple; P, orange; O, red; C, grey; H, white. H-bonding, green line; $CH_3-\pi$ interactions, blue line. Hydrogen atoms, except for the triol, and acetonitrile solvent molecules are omitted for clarity.

Table 1. Results of ITC titrations of **Tiiii[C$_3$H$_7$, CH$_3$, Ph]**, **Tiiii[C$_3$H$_7$, H, Ph]** and **TSiiii[C$_3$H$_7$, H, Ph]** with **2** and **3** in DCE and in CH$_3$OH at 303 K.

Entry	Host	Guest	Solvent	$K_{ass} \pm \delta K_{ass}$ (M^{-1})	$\Delta H \pm \delta H$ (kJ·mol^{-1})	ΔG (kJ·mol^{-1})	$T\Delta S$ (kJ·mol^{-1})
I	**Tiiii[C$_3$H$_7$, CH$_3$, Ph]**	2	MeOH	$3.4 \pm 0.3 \times 10^4$	-17.2 ± 0.3	-26.3 ± 0.3	9.1 ± 0.1
II		2	DCE	$5.8 \pm 0.6 \times 10^6$	-25.7 ± 0.2	-39.2 ± 1.4	13.5 ± 2.4
		3	MeOH	$3.9 \pm 0.1 \times 10^4$	-11.3 ± 0.1	-26.7 ± 0.1	15.4 ± 0.1
		3	DCE	$3.1 \pm 0.3 \times 10^6$	-20.9 ± 0.1	-37.7 ± 0.1	16.8 ± 0.2
III	**Tiiii[C$_3$H$_7$, H, Ph]**	2	DCE	$2.8 \pm 0.4 \times 10^5$	-8.2 ± 0.2	-31.6 ± 0.1	23.4 ± 0.2
IV		3	DCE	$1.3 \pm 0.4 \times 10^5$	-6.8 ± 0.2	-29.7 ± 2.1	22.9 ± 3.9
V	**TSiiii[C$_3$H$_7$, H, Ph]**	2	DCE	No interaction detectable			
VI		3	DCE	No interaction detectable			

typical columnar disposition along the *a*-axis of the unit cell (see Figure 1, right). The distance between I^- and the positive nitrogen of the guest is 7.679(3) Å. All the above values are in good agreement with similar complexes reported in the literature (*2*, *14*).

The first set of ITC measurements was made to assess the solvent effect on the complexation. For this purpose, dichloroethane (DCE) and methanol were chosen. The former does not compete for the cavity due to its size and its low propensity to form hydrogen bonds with the P=O units of the cavitand. Vice versa, in the case of methanol, crystal structures showed its inclusion in the cavity of Tiiii receptors (*10*), driven by the synergistic action of H-bonding with the phosphonates and $CH_3-\pi$ interactions with the cavity. The different affinity of the two solvents for the cavity is clearly reflected in the complexation of guests **2** and **3** by **Tiiii[C$_3$H$_7$, CH$_3$, Ph]**. A decrease of the association constant of two orders of magnitude was determined for both guests by moving from DCE to MeOH (Table 1, entries I and II). In both cases, the reduced affinity in MeOH is mainly enthalpic in origin, with the ΔH reduction attributable to the solvent competition for the cavity and the electrostatic stabilisation of the cationic guest by the more polar solvent. Interestingly, the counterion does not influence complexation, leading to comparable values of ΔG and K_{ass}. Such unexpected silence in impact may be attributed to the preferential positioning of both iodide and PF_6^- within the alkyl chains, as was proven in NMR studies in chloroform (*14*). Yet, the absence of evidence of a role for the counterions in the binding process can also arise from an adventitious cancellation of enthalpic and entropic effects of complexation at the less structured, well-solvated and solvent-like site of the host compound.

Next, the role of the cavity structure on complexation was investigated. The presence of four methyl groups in the apical positions of **Tiiii[C$_3$H$_7$, CH$_3$, Ph]** deepens the cavity and enhances its π-basic character. Their removal should reduce the complexation efficiency of the receptor. Experimentally, a decrease of the K_{ass} of one order of magnitude was observed for the titration of methyl-depleted cavitand **Tiiii[C$_3$H$_7$, H, Ph]** with guests **2** and **3** in DCE, as compared to the original ones (Table 1, compare entry I with entry III, and entry II with entry IV).

A large enthalpic drop was determined, only partially compensated by an entropic gain. This is ascribed to the reduced contribution of $CH_3-\pi$ interactions (*15*) to the overall binding and to the enhanced solvation of the more open cavity of the demethylated host **Tiiii[C$_3$H$_7$, H, Ph]**. The latter origin is also suggested by the entropic outcome which testifies to more dramatic cavity desolvation and guest mobility in the case of **Tiiii[C$_3$-H$_7$, H, Ph]** upon binding, while the guest desolvation is comparable in the two cases. It is worth noting that the methylpyridinium binding remains both enthalpy and entropy driven. As shown in Table 1 (entries III and IV), the thermodynamic parameters of **Tiiii[C$_3$H$_7$, H, Ph]** complexation in DCE are not influenced by the counterions, confirming the results reported for the parent **Tiiii[C$_3$H$_7$, CH$_3$, Ph]**.

In order to probe the contribution of cation–dipole interactions on the overall binding, tetrathiophosphonate cavitand **TSiiii[C$_3$H$_7$, H, Ph]** was prepared (Scheme 1). It is structurally identical to the corresponding tetraphosphonate **Tiiii[C$_3$H$_7$, H, Ph]**, except for the presence of four inward-facing P=S instead of four P=O bridging units. The P=S group is more polarisable than the P=O counterpart, but it has a much smaller dipole moment (*16*). Its larger size does not preclude the insertion of methyl groups into the cavity (*17*); therefore, the introduction of four P=S bridges has little influence on $CH-\pi$ interactions. As a corollary, this substitution should decrease substantially the cation–dipole interactions with the charged methylpyridinium guests. The ITC results were beyond our expectations: the affinity of the cavitand for guests **2** and **3** was completely shut off (Table 1, entries V and VI). Therefore, the cation–dipole interactions are indispensable for binding methylpyridinium guests. Without P=O, the complexation is negligible, well below the detection limit of ITC.

3. Conclusions

The selective complexation of methylpyridinium salts by tetraphosphonate cavitands relies on two interactions, namely cation–dipole and $CH_3-\pi$, which operate synergically. The crystal structure of the reported complex clearly evidences this synergy in the solid state. Using ITC, the thermodynamic profile in the formation of several host–guest complexes was determined. They all are driven both by enthalpy and entropy (*18*, *19*), reflecting the importance and substantial participation of solvent interactions for the binding process. The relative weights of the two direct mutual interaction modes have been dissected by changing two structural parameters on the cavitands. The dominant role of cation–dipole interactions was revealed by substituting the P=O bridges with the P=S ones, which completely suppressed complexation. The relevance of $CH-\pi$ interactions was highlighted by the removal of the four methyl groups in the cavity apical positions, which led to the decrease of one order of magnitude in the K_{ass} of both **2** and **3**. On the guest side, the counterion does not play a significant role in complexation, which can be due to an adventitious cancellation of effects, but may also emerge from the basic lack of binding. The solvent instead affects the binding significantly, particularly when the solvent competes with the guest for the cavity space, like in the case of methanol.

4. Experimental

4.1 General methods

All commercial reagents were ACS reagent grade and were used as received, except for 4-picoline which was purified by fractional distillation before use. Solvents were dried and distilled using standard procedures. ^{1}H NMR spectra were recorded on Bruker Avance 300 (300 MHz) and on Bruker FT-DPX b200 NMR spectrometers. All chemical shifts (δ) were reported in parts per million (ppm) relative to proton resonances resulting from incomplete deuteration of NMR solvents. ^{31}P NMR spectra were recorded on AMX-400 (162 MHz), and all chemical shifts were reported to external 85% H_3PO_3 at 0 ppm. Electrospray ionisation mass spectrometry (ESI-MS) experiments were performed on a Waters ACQUI-LITY UPLC SQ Detector. ITC measurements were performed with a fully computer-operated MicroCal ITC-MCS instrument at 303 K by adding 2–10 μL aliquots of the guest solution into the thermostated solution of the host compound present in about 10-fold lower concentration in the calorimetric cell (1.35 mL).

To obtain a good quality data output, it is essential to choose the best experimental conditions. One adjustable parameter that needs optimal setting is the c parameter:

$$c = n \times [A]K_{ass},$$

where n is the stoichiometric factor, $[A]$ is the concentration of the titrate compound in the cell (M) and K_{ass} is the affinity constant (M^{-1}). In order to obtain a sigmoidal output curve from which the K_{ass}, the stoichiometric factor n and the ΔH are derived, the c parameter should be set within the range 5–500. Adjusting the titrate concentration is the key factor to reach a good shaped curve.

Cavitand **Tiiii[C_3H_7, CH_3, Ph]** (*11*), resorcinarene **Res[C_3H_7, H]** (*20*), and guests **2** (*3*) and **3** (*11*) were prepared following a published procedure.

4.2 Cavitand T$_{iiii}$[C_3H_7, H, Ph]

To a solution of resorcinarene **Res[C_3H_7, H]** (517 mg, 0.80 mmol) in freshly distilled pyridine (20 mL), dichlorophenylphosphine (0.447 mL, 3.39 mmol) was added slowly at room temperature. After 3 h of stirring at 80°C, the solution was allowed to cool to room temperature, and 8 mL of a mixture of 35% H_2O_2 and $CHCl_3$ (1:1) was added. The resulting mixture was stirred for 30 min at room temperature; then, the solvent was removed under reduced pressure and water was added. The precipitate obtained in this way was collected by vacuum filtration, and purified by recrystallisation (H_2O:CH_3CN 8:2). The product is a fine white powder (870 mg, 95%).

^{1}H NMR (300 MHz, $CDCl_3$): δ (ppm) 8.09 (m, 8H, POArH_o); 7.61 (m, 4H, POArH_p); 7.52 (m, 8H, POArH_m); 7.13 (s, 4H, ArH_{down}); 6.51 (s, 4H, ArH_{up}); 4.81 (t, 4H, $J = 7.4$ Hz, ArCH); 2.34–2.20 (m, 8H, CH_2CH$_2$CH$_3$); 1.41 (m, 8H, CH$_2$CH_2CH$_3$); 1.04 (t, 12H, $J = 7.4$ Hz, CH$_2$CH$_2$CH_3). ^{31}P NMR (162 MHz, $CDCl_3$) δ (ppm): 4.02 (s, 4P). ESI-MS: *m/z* 1167.3 [M + Na]$^+$.

4.3 Cavitand TSiiii[C_3H_7, H, Ph]

To a solution of resorcinarene **Res[C_3H_7, H]** (2.26 g, 3.5 mmol) dissolved in 20 mL of freshly distilled pyridine, dichlorophenylphosphine (1.93 mL, 14.3 mmol) was slowly added at room temperature. The mixture was stirred for 3 h at 80°C and then cooled to room temperature. S_8 (0.72 g, 2.81 mmol) was added and left stirring for 1 h at 50°C. The solvent was removed in vacuum followed by the addition of 50 mL of water, and the yellow suspension was filtered. Purification by column chromatography on silica gel with CH_2Cl_2:hexane (9/1 v/v) yielded the product (2.62 g, 62%).

^{1}H NMR (300 MHz, $CDCl_3$): δ (ppm) 8.19 (m, 8H, POArH_o); 7.60 (m, 4H, POArH_p); 7.51 (m, 8H, POArH_m); 7.21 (s, 4H, ArH_{down}); 6.50 (s, 4H, ArH_{up}); 4.72 (t, 4H, $J = 7.8$–Hz, ArCH); 2.31 (m, 8H, CH_2CH$_2$CH$_3$); 1.40 (m, 8H, CH$_2$CH_2CH$_3$); 1.02 (t, 12H, $J = 7.2$–Hz, CH$_2$CH$_2$-CH_3). ^{31}P NMR: (172 MHz, $CDCl_3$): δ (ppm) 72(s, 4P). ESI-MS: *m/z*: 1231.3 [M + Na]$^+$.

4.4 2-(Hydroxymethyl)-2-(pyridin-4-yl)-1,3-propanediol (I)

The following procedure (Scheme 2) improves the method proposed by Koenigs and Happe (*21*). 4-Picoline (2.00 g, 21.5 mmol) was refluxed in 37% aqueous formaldehyde (27 mL, 360 mmol) for 24 h. The solvent and excess formaldehyde were removed under reduced pressure at 50°C. Methanol (50 mL) was added to the residue and removed under vacuum at 50°C, and the procedure was repeated. The crude product was subjected to prolonged vacuum pumping (1 mmHg, 3 h), and purified by column chromatography (CH_2Cl_2:CH_3OH 8/2 v/v) to afford the
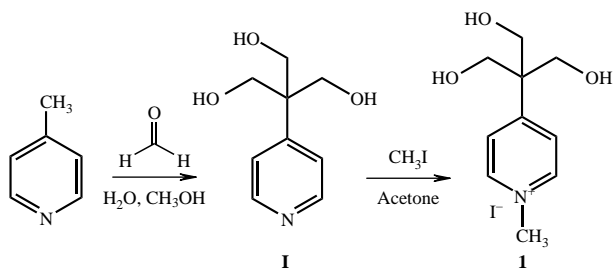
Scheme 2. Synthesis of triol guest **1**.

desired compound as a white crystalline solid (2.25 g, 57%).

¹H NMR (200 MHz, CD₃OD): δ (ppm) 3.93 (s, 6H, C*H₂*); 7.54 (m, 2H, C*H* meta to N); 8.45 (m, 2H, C*H* ortho to N).

4.5 4-[1,3-Dihydroxy-2-(hydroxymethyl)propan-2-yl]-1-methylpyridinium iodide (1)

Compound **I** (0.100 g, 0.546 mmol) was suspended in acetone (3 mL), and MeI (50 μL, 0.80 mmol) was added. The mixture was stirred overnight at 40–45°C in a closed glass tube, cooled down to room temperature and concentrated. The off-white solid so obtained was separated by filtration and dried under vacuum (163 mg, 92%).

¹H NMR (200 MHz, CD₃OD): δ (ppm) 3.97 (s, 6H, C*H₂*); 4.38 (s, 3H, C*H₃*); 8.23 (m, 2H, C*H* meta to N); 8.80 (m, 2H, C*H* ortho to N).

4.6 Crystal structure determination of the Tiiii[C₃H₇, CH₃, Ph]·(C₁₀H₁₆INO₃)·5CH₃CN complex

The molecular structure of the inclusion compound **Tiiii[C₃H₇, CH₃, Ph]·(C₁₀H₁₆INO₃)·5CH₃CN** was determined by single-crystal X-ray diffraction methods. Crystallographic and experimental details are summarised

Table 2. Crystallographic data and refinement details for compound **Tiiii[C₃H₇, CH₃, Ph]·(C₁₀H₁₆INO₃)·5CH₃CN**.

	Tiiii[C₃H₇, CH₃, Ph]·(C₁₀H₁₆INO₃)·5CH₃CN
Formula	$C_{88}H_{99}IN_6O_{15}P_4$
Formula weight	1731.51
Crystal system	Monoclinic
Space group	*P2₁/c*
a (Å)	15.479 (3)
b (Å)	37.943 (6)
c (Å)	16.352 (3)
β (°)	113.988 (2)
V (Å³)	8775 (2)
Z	4
D_c (g cm⁻³)	1.311
$F(000)$	3608
μ (mm⁻¹)	0.504
$\theta_{min,max}$ (°)	1.07, 28.56
Reflections collected	71,985
Independent reflections	19711 ($R_{int} = 0.0384$)
Obs. refl. [$I > 2\sigma(I)$]	13,715
Data/restr./param.	19,711/0/950
R indices [$I > 2\sigma(I)$]ᵃ	$R_1 = 0.0484$, $wR_2 = 0.1296$
R indices (all data)	$R_1 = 0.075$, $wR_2 = 0.1420$
$\Delta\rho_{min,max}$/e Å⁻³	−1.097, 0.827
S^b	1.002

ᵃ $R_1 = \Sigma||F_o| - |F_c||/\Sigma|F_o|$, $wR_2 = [\Sigma w(F_o^2 - F_c^2)^2/\Sigma wF_o^4]^{1/2}$.
ᵇ Goodness-of-fit $S = [\Sigma w(F_o^2 - F_c^2)^2/(n - p)]^{1/2}$, where *n* is the number of reflections and *p* is the number of parameters.

in Table 2. Intensity data and cell parameters were recorded at 173 K on a Bruker AXS Smart 1000 single-crystal diffractometer (employing a MoK$_\alpha$ radiation and a CCD area detector). The raw frame data were processed using SAINT and SADABS to yield the reflection data file (*22*). The structure was solved by direct methods using the SIR97 program (*23*), and refined on F_o^2 by full-matrix least-squares procedures using the SHELXL-97 program (*24*). The PLATON/SQUEEZE procedure (*25*) was used to treat regions of diffuse solvent, which could not be sensibly modelled in terms of atomic sites. Their contribution to the diffraction pattern was removed, and modified F_o^2 was written on a new HKL file. The 275 electrons per unit cell thus located are included in the formula, formula weight, calculated density, μ and $F(000)$. This residual electron density was assigned to 12 molecules of acetonitrile per unit cell. All non-hydrogen atoms were refined with anisotropic atomic displacements with the exception of one acetonitrile molecule. The hydrogen atoms were included in the refinement at idealised geometry (C—H 0.95Å) and refined 'riding' on the corresponding parent atoms.

The weighting schemes used in the last cycle of refinement were $w = 1/[\sigma^2 F_o^2 + (0.0848P)^2 + 1.4464P]$, where $P = (F_o^2 + 2F_c^2)/3$. Molecular geometry calculations were carried out using the PARST97 program (*26*). Drawings were obtained using ORTEP3 in the WinGX suite (*27*) and Mercury (*28*). Crystallographic data (excluding structure factors) for the structure reported have been deposited with the Cambridge Crystallographic Data Center as supplementary publication no. CCDC-777331, and can be obtained free of charge on application to the CCDC, 12 Union Road, Cambridge CB2 1EZ, UK. [Fax: +44-1223/336-033; deposit@ccdc.cam.ac.uk].

References

(1) Dutasta, J.-P. *Top. Curr. Chem.* **2004**, *232*, 55–91.
(2) Biavardi, E.; Favazza, M.; Motta, A.; Fragalà, I.L.; Massera, C.; Prodi, L.; Montalti, M.; Melegari, M.; Condorelli, G.G.; Dalcanale, E. *J. Am. Chem. Soc.* **2009**, *131*, 7447–7455.
(3) Tancini, F.; Genovese, D.; Montalti, M.; Cristofolini, L.; Nasi, L.; Prodi, L.; Dalcanale, E. *J. Am. Chem. Soc.* **2010**, *132*, 4781–4789.
(4) Yebeutchou, R.M.; Tancini, F.; Demitri, N.; Geremia, S.; Mendichi, R.; Dalcanale, E. *Angew. Chem., Int. Ed.* **2008**, *47*, 4504–4508.
(5) Lippmann, T.; Mann, G.; Dalcanale, E. *Tetrahedron Lett.* **1994**, *35*, 1685–1688.
(6) Delangle, P.; Dutasta, J.-P. *Tetrahedron Lett.* **1995**, *36*, 9325–9328.

(7) For the nomenclature adopted for phosphonate cavitands see Pinalli, R.; Suman, M.; Dalcanale, E. *Eur. J. Org. Chem.* **2004**, 451–462.

(8) Delangle, P.; Mulatier, J.-C.; Tinant, B.; Declercq, J.-P.; Dutasta, J.-P. *Eur. J. Org. Chem.* **2001**, *66*, 3695–3704.

(9) Kalenius, E.; Moiani, D.; Dalcanale, E.; Vainiotalo, P. *Chem. Commun.* **2007**, 3865–3867.

(10) Melegari, M.; Suman, M.; Pirondini, L.; Moiani, D.; Massera, C.; Ugozzoli, F.; Kalenius, E.; Vainiotalo, P.; Mulatier, J.-C.; Dutasta, J.-P.; Dalcanale, E. *Chem. Eur. J.* **2008**, *14*, 5772–5779.

(11) Biavardi, E.; Battistini, G.; Montalti, M.; Yebeutchou, R.M.; Prodi, L.; Dalcanale, E. *Chem. Commun.* **2008**, 1638–1640.

(12) Sessler, J.L.; Gross, D.E.; Cho, W.-S.; Lynch, V.M.; Schmidtchen, F.P.; Bates, G.W.; Light, M.E.; Gale, P.A. *J. Am. Chem. Soc.* **2006**, *128*, 12281–12288.

(13) Schmidtchen, F.P. In *Analytical Methods in Supramolecular Chemistry*; Shalley, C.A., Ed.; Wiley; Verlag GmbH & Co. KGaA: Weinheim, Germany, 2007; pp 55–78.

(14) De Zorzi, R.; Dubessy, B.; Mulatier, J.-C.; Geremia, S.; Randaccio, L.; Dutasta, J.-P. *J. Org. Chem.* **2007**, *72*, 4528–4531.

(15) For selected references of CH–π interactions see: (a) Nishio, M.; Hirota, M.; Umezawa, Y. *The CH–π Interactions*, Wiley, New York, 1998. (b) Dougherty, D.A.; Stauffer, D.A. *Science* **1990,** *250*, 1558–1560. (c) Kim, E.-i-; Paliwal, S.; Wilcox, C.S. *J. Am. Chem. Soc.* **1995**, *120*, 11192–11193. (d) Piatnitski, E.L.; Flowers II, R.A.; Deshayes, K. *Chem. Eur. J.* **2000**, *6*, 999–1006.

(16) Hawkins, N.J.; Cohen, V.W. *J. Chem. Phys.* **1952**, *20*, 528.

(17) The crystal structure of TSiiii[C$_3$H$_7$, H, Ph]·CH$_3$CN with acetonitrile included in the cavity has been determined (S. Geremia, M. Melegari, E. Dalcanale. unpublished results).

(18) Moghaddam, S.; Inoue, Y.; Gilson, M.K. *J. Am. Chem. Soc.* **2009**, *131*, 4012–4021.

(19) Schmidtchen, F.P. *Coord. Chem. Rev.* **2006**, *250*, 2918–2928.

(20) Tunstad, L.M.; Tucker, J.A.; Dalcanale, E.; Weiser, J.; Bryant, J.A.; Sherman, J.C.; Hegelson, R.C.; Knobler, C.B.; Cram, D.J. *J. Org. Chem.* **1989**, *54*, 1305–1312.

(21) Koenigs, W.; Happe, G. *Ber. Dtsch. Chem. Ges.* **1903**, *36*, 2904–2912.

(22) SADABS Bruker AXS; Madison, Wisconsin, USA, 2004; SAINT, Software Users Guide, Version 6.0; Bruker Analytical X-ray Systems. In *Software Users Guide*, Version 6.0; Bruker *Analytical X-ray Systems*, Madison, WI, 1999. Sheldrick, G.M.; *SADABS v2.03: Area-Detector Absorption Correction*. University of Göttingen, Germany, 1999.

(23) Altomare, A.; Burla, M.C.; Camalli, M.; Cascarano, G.L.; Giacovazzo, C.; Guagliardi, A.; Moliterni, A.G.G.; Polidori, G.; Spagna, R. *J. Appl. Crystallogr.* **1999**, *32*, 115–119.

(24) Sheldrick, G.M.; *SHELXL97. Program for Crystal Structure Refinement*, University of Göttingen: Göttingen, Germany, 1997; Sheldrick, G.M. *Acta Cryst.*, **2008,** *A64*, 112–122.

(25) SQUEEZE – v.d Sluis P.Spek, A.L. *Acta Crystallogr., Sect A* **1990**, *46*, 194–201.

(26) PARST – (a) Nardelli, M. *Comput. Chem.* **1983,** *7*, 95–97. (b) Nardelli, M. *J. Appl. Crystallogr.* **1996**, *29*, 296–300.

(27) ORTEP3 for Windows-Farrugia, L.J. *J. Appl. Crystallogr.* **1997**, *30*, 565.

(28) Mercury CSD 2.2 (Build RC5).